Catalysis Science & Technology

Accepted Manuscript

ROYAL SOCIETY OF CHEMISTRY

www.rsc.org/catalysis

Graphical abstract:

Incorporation of Zn^{2+} ions into the secondary structure of heteropoly tungstate: Catalytic efficiency for synthesis of glycerol carbonate from glycerol and urea

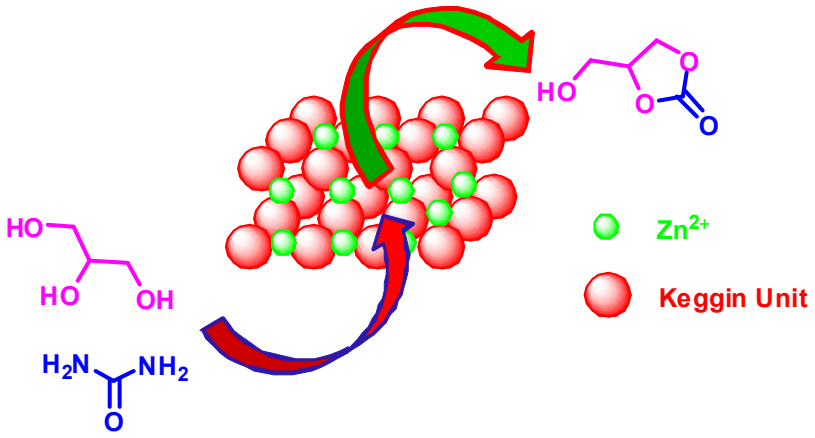

Incorporation of Zn^{2+} ions into the secondary structure of heteropoly tungstate: Catalytic efficiency for synthesis of glycerol carbonate from glycerol and urea

K. Jagadeeswaraiah, Ch. Ramesh Kumar, P.S. Sai Prasad and N. Lingaiah*

Catalysis Laboratory, Inorganic & Physical Chemistry Division,

CSIR-Indian Institute of Chemical Technology, Hyderabad-500 007, India.

Abstract

Zinc exchanged heteropoly tungstate (Zn_xTPA) catalysts were prepared and characterized by FT–IR, X–ray diffraction, Laser Raman, temperature programmed desorption of ammonia and pyridine adsorbed FT–IR spectroscopy. The activity of the catalysts was evaluated for the carbonylation of glycerol using urea as a carbonylating agent. Zn_xTPA catalysts showed high activity for glycerol carbonate synthesis compared to parent TPA. The activity of Zn_xTPA catalysts depended on the number of Zn^{2+} ions in the secondary structure of heteropoly tungstate. Catalyst with partial exchange of Zn with the protons of TPA (Zn_1TPA) exhibited high activity towards glycerol carbonate synthesis. Exchange of protons of TPA with Zn^{2+} ions resulted in generation of Lewis acidic sites. The surface and structural properties of Zn_1TPA catalyst with change in calcination temperature were also evaluated. The catalytic activities of Zn_xTPA catalysts were explained on the variation in their properties. Reaction conditions such as reaction temperature, catalyst weight and glycerol to urea ratio were also optimized.

Keywords: Carbonylation; Glycerol; Glycerol carbonate; Heteropoly tungstate; Urea; Zinc

*Corresponding Author; Phone: +91–40–27191722; Fax: +91–40–27160921

E-mail address: nakkalingaiah@iict.res.in (N. Lingaiah)

Introduction

Glycerol is a major by–product in the production of biodiesel by the transesterification of oils and fats. High production of biodiesel in recent times resulted in a surplus of glycerol as its traditional requirements in the chemical, food, pharmaceutical and cosmetics industries is limited.[1–3] Glycerol is used as a raw material in several fields like pharmaceutics, cosmetics, food industry, explosives production, as a green solvent.[4–6] The transformation of glycerol to value–added chemicals is one approach to address the surplus of glycerol. Glycerol can be converted into different chemicals by selective oxidation,[7] hydrogenolysis,[8] dehydration,[9] transesterification, esterification,[10,11] carbonylation,[12–14] and etherification.[15] Among the different glycerol derivatives, glycerol carbonate (4–hydroxymethyl–1,3–dioxolan–2–one) is one of the most promising chemical,[11] due to its ideal physico chemical properties. Glycerol carbonate has many applications in the synthesis of polycarbonates, polyurethanes, surfactants, pharmaceuticals and cosmetics.[16,17]

Several routes have been reported for the synthesis of glycerol carbonate from glycerol using different carbonyl sources.[16,18–22] Glycerol carbonate can be prepared by i) transesterification of glycerol with dialkyl carbonates,[10] ii) reaction of glycerol with carbon monoxide and oxygen,[12,13,19] iii) reaction of glycerol with carbon dioxide,[18] iv) from glycerol and phosgene,[23] and v) reaction of glycerol with urea.[10, 14,24–26]

Use of carbon monoxide and phosgene as a carbonylating agent is limited due to the toxicity and difficult to handle in industries.[17,21] Carbonylation of glycerol with CO_2 is best approach.[18,27] The main drawback of this reaction that the overall yield of glycerol carbonate is very less.

The use of alkyl carbonates like ethylene carbonate as carbonylating agent is also a useful approach. However, glycerol carbonate is obtained along with ethylene glycol. The separation of by–product is difficult.[10] The use of dimethyl carbonate as carbonate source requires use of base catalysts such K_2CO_3 and CaO.[20,28] However, these catalysts often lose their activity after first use.

One of the practical routes for carbonylation of glycerol is the use of urea as carbonate source.[26] The major advantage of this method over other processes is that urea is readily available and cheap, the by–product produced in this reaction (ammonia) can be utilized for the synthesis of urea. From the literature it is noted that catalysts with Lewis acidic sites such as, ZnO,[22,29,30] zinc sulfate,[29] $ZnCl_2$,[31] γ–zirconium phosphate,[25] mixed metal oxides,[14] HTc–Zn derived from hydrotalcite,[10] Co_3O_4/ZnO,[32] Sm exchanged heteropoly tungstate,[24] gold supported ZSM–5,[26] manganese sulfate,[26] etc. produces high glycerol carbonate yields.

Recently, use of metal exchanged 12–tungstophosphoric acid as solid acid catalysts has been developed for acid catalyzed reactions due to their unique acidic properties.[24,33,34] Exchange of protons with certain metal ions generates Lewis acid sites.[35] Since Zn^{2+} is a Lewis acid and can be used to exchange the protons of tungstophosphoric acid (TPA) to generate Lewis acidity. Zinc oxide based catalysts have been proved to be useful catalysts[22,29,30] for the carbonylation of glycerol. Li *et al.* reported the synthesis of $Zn_{1.2}H_{0.6}PW_{12}O_{40}$ nano tubes and the catalytic activity was evaluated for the production of biodiesel.[33] However, variation in acidity with increase in Zn content in secondary structure of tungstophosphoric acid and their detail characterization was not studied.

In the present work, a series of zinc exchanged tungstophosphoric acid (Zn_xTPA) catalysts were prepared by exchanging the protons of TPA with Zn^{2+} ions. The catalytic

activities of these catalysts were tested for the synthesis of glycerol carbonate from glycerol and urea. The physico–chemical properties of the Zn_xTPA catalysts with varying of Zn content and treatment temperature were derived and correlated with the catalytic activity.

Experimental

Preparation of zinc exchanged TPA catalysts

Zn exchanged TPA catalysts were prepared by titration method as reported in the literature.[24] The required quantity of TPA dissolved in minimum amount of distilled water and to this calculated amount of aqueous $Zn(NO_3)_2$ solution was added drop wise. The resulting mixture was aged for 1 h at 80 °C. The excess water was evaporated to dryness on water bath. The obtained catalyst mass was oven dried at 120 °C for overnight and calcined at 300 °C for 2 h. The catalysts were designed as Zn_xTPA, where x= 0.5, 1, and 1.5. Zn_1TPA catalyst calcined at different temperatures ranging from 300 to 600 °C. These catalysts are denoted as Zn_1TPA-300 to 600. The number indicates the calcination temperature.

Characterization of catalysts

Fourier transform infrared (FT–IR) spectra were recorded on a Bio–rad Excalibur series spectrometer using KBr disc method.

The nature of the acid sites (Bronsted and Lewis) of the catalysts was determined by FT–IR spectroscopy with chemisorbed pyridine. The pyridine adsorption studies were carried out in the diffuse reflectance infrared Fourier transform (DRIFT) mode. Prior to the pyridine adsorption catalysts were degassed under vacuum at 200 °C for 3 h followed by suspending dry pyridine. Then, the excess pyridine was removed by heating the sample at 120 °C for 1 h. After cooling the sample to room temperature, FT–IR spectra of the pyridine–adsorbed samples were recorded.

X–ray powder diffraction patterns were recorded on a Rigaku Miniflex diffractometer using Cu K_α radiation (1.5406 °A) at 40 kV and 30 mA and secondary graphite monochromatic. The measurements were obtained in steps of 0.045 ° with count times of 0.5 S, in the 2θ range of 5–80°.

Confocal Micro–Raman spectra were recorded at room temperature in the range of 200–1200 cm^{-1} using Horiba Jobin–Yvon Lab Ram HR spectrometer with a 17 mW internal He–Ne (Helium–Neon) laser source of excitation wavelength of 632.8 nm. The catalyst samples in powder form (about 5–10 mg) were usually loosely spread onto a glass slide below the confocal microscope for measurements.

The acidity of the catalysts was measured by temperature programmed desorption of ammonia (TPD–NH_3). In a typical experiment, 0.1 g of catalyst was loaded and pre–treated in He gas at 300 °C for 2 h. After pre–treatment the temperature was brought to 100 °C and the adsorption of NH_3 was carried out by passing a mixture of 10% NH_3 balanced He gas over the catalyst for 1h. The catalyst surface was flushed with He gas at the same temperature for 2 h to flush off physisorbed NH_3. TPD of NH_3 was carried with a temperature ramp of 10 °C/min and the desorbed ammonia was monitored using thermal conductivity detector (TCD) of a gas chromatograph.

Synthesis of glycerol carbonate

The reactions were performed in a 25 mL two neck round–bottom (RB) flask under reduced pressures. In a typical experiment, glycerol (2 g), urea (1.306 g) and catalyst (0.2 g) were taken in the round bottom flask and heated in an oil bath at 140 ^oC with constant stirring. One neck of the RB flask was connected to vacuum line. Reaction was run under a reduced pressure in order to remove ammonia formed during the reaction. After completion of the

reaction or stipulated time, methanol was added and the catalyst was separated by filtration. The products were analyzed by a gas chromatograph (Shimadzu 2010) equipped with flame ionization detector using inno wax capillary column (diameter: 0.25 mm, length 30 m). Products were also identified by GC–MS (Shimadzu, GCMS–QP2010S) analysis.

Results and discussion

Catalyst characterization

Structural and surface characteristics of Zn_xTPA catalysts were evaluated by different spectroscopic and non spectroscopic techniques such as, X–ray diffraction, FT–IR spectroscopy, Laser Raman, TPD of ammonia and pyridine adsorbed FT–IR spectroscopy.

XRD patterns

XRD patterns of Zn_xTPA catalysts along with pure TPA are shown in Figure 1. Pure TPA showed characteristic XRD patterns of Keggin ion at 2θ values of 10.28°, 17.93°, 23.13°, 25.42°, 29.49°, 37.74°.[34] All the catalysts showed the characteristic XRD patterns related to Keggin ion of heteropoly tungstate. However, in the case of Zn_xTPA catalysts with increase in Zn content from 0.5 to 1.5, intensities of the characteristic diffraction peaks related to Keggin ion were decreased and additional peaks were observed. This result suggests that the Zn_xTPA catalysts consist of parent TPA and crystalline salt of Zn_xTPA. From the literature it is observed a shift in XRD patterns when the protons of TPA exchanged with metal ions such as Sm^{3+} and Cs^{+}.[24,36] Similarly, in the case of Zn_xTPA catalysts with increase in Zn content from 0.5 to 1, intensity of the characteristic peak at 10.28° decreased and shifted to lower angles at 8.86°. Further increase in Zn content characteristic peak at 10.28° is completely disappeared and which indicates an expansion of unit cell volume.[24]

Fourier Transform Infrared spectroscopy

FT–IR spectra of bulk TPA and Zn exchanged tungstophosphoric acid catalysts are shown in Figure 2. TPA exhibited four bands in the finger print region 1100–500 cm^{-1}. The characteristic Keggin ion peaks of TPA observed at 1082, 988, 890, and 792 cm^{-1} were attributed to P–O_a (O_a– oxygen atom bound to three W atoms and to P), W=O_t (t– terminal oxygen), W–O_c–W (O_c– corner sharing bridging oxygen atom), and W–O_e–W (O_e– an edge–sharing bridging oxygen atom), respectively.[37] All the Zn_xTPA catalysts showed the characteristic bands of Keggin heteropoly tungstate indicates that primary Keggin structure remained unchanged even after exchanging the protons of TPA with Zn^{2+} ions.

Laser Raman spectroscopic studies

Figure 3 shows the Raman spectra of Zn_xTPA catalysts along with bulk TPA. Pure crystalline TPA showed characteristic bands at 1015, 990, 933, 530, 231, and 215 cm^{-1}.[38] The bands at 1015 and 990 cm^{-1} are asymmetric and symmetric vibrations of W=O_t, respectively. The Raman bands at 933 and 530 are ascribed to asymmetric and symmetric stretching vibrations of W–O_c–W and W–O_e–W, respectively. The band observed at 231 cm^{-1} is related to W–O–W bending mode and the band at 215 cm^{-1} might be due to the coupling between two bending mode vibrations.[34] Zn exchanged heteropoly tungstate catalysts also showed all the characteristic bands related to the Keggin ion, confirming the existence of the primary Keggin structure of heteropoly tungstate.

Temperature programmed desorption of ammonia

Acidity of the Zn_xTPA catalysts were measured by TPD of NH_3 and the patterns are shown in Figure 4. The acidity values calculated based on desorbed ammonia are presented in Table 1. The patterns showed three desorption peaks in the range of 120–700 °C. The main desorption

peaks observed in the range of 120–300 °C and 300–450 °C corresponding to weak and moderate acidic sites, respectively. Another strong desorption peak observed in the range of 450–700 °C related to strong acidic sites. With increase in exchangeable Zn ions from 0.5 to 1, the desorption peak related to strong acidic sites shifted to lower temperatures and intensity of the desorption peak corresponding to weak acidic sites is increased. Further increase in Zn content to 1.5, intensity of the desorption peak related to strong acidic sites decreased and at the same time intensity of the desorption peak related to moderate acidic sites also increased. This suggested that the number of moderate acidic sites, which are probably Lewis acidic, increased with Zn content (Table 1). Compared to other catalysts partially exchanged Zn_1TPA catalyst exhibited high acidity.

FT–IR pyridine adsorption studies

Pyridine adsorbed FT–IR spectroscopy can used to investigate the presence of Bronsted and Lewis acidic sites in a catalyst. Pyridine adsorbed FT–IR spectra of Zn_xTPA catalysts are shown in Figure 5. The pyridine–adsorbed FT–IR spectra showed various features in the region of 1400–1600 cm^{-1} due to the stretching vibrations of M–N (metal–nitrogen) and N–H (pyridinium ion). The band assigned to the pyridinium ion is recorded at 1536 cm^{-1} and the other one at 1449 cm^{-1} associated to pyridine adsorbed onto Lewis–type acid sites. The FT–IR spectra of TPA shows typically intense bands at 1530, and 1542 cm^{-1} characteristic of Bronsted acidic sites.[39] Another intense band at 1485 cm^{-1}, which is a combined band originating from pyridine bonded to both the Bronsted and Lewis acid sites.[33] In the case of Zn exchanged TPA catalysts, the band related to Lewis acidic site is clearly seen at 1448 cm^{-1} and its intensity increased with increase in Zn content in the sample. Intensity of the band related to Bronsted acidic sites decreased with increase in Zn content indicating the generation of Lewis acidic sites in Zn_xTPA

catalysts. TPD of NH_3 results also supports the presence of Lewis acidic sites as Zn_xTPA (x=0.5–1.5) catalysts exhibited a strong desorption peak related to moderate acidic sites.

Activity measurements

Preparation of glycerol carbonate from urea and glycerol

The activity of zinc exchanged tungstophosphoric acid catalysts was evaluated for the synthesis of glycerol carbonate and the results are presented in Table 2. The catalytic activity of ZnO was also studied for comparison. When reaction was carried in the absence of catalyst, conversion of glycerol was only 10.5% and selectivity towards glycerol carbonate was 19.3%. However, in the presence of ZnO conversion of glycerol is improved to 34% with 91.2% selectivity towards glycerol carbonate. However, the TPA showed about 40% glycerol conversion with 75.7% selectivity towards glycerol carbonate. The exchange of Zn with the protons of TPA resulted a substantial enhancement in activity. The presence of Zn led to an increase in glycerol conversion from 40.4% to 60.4%. Further increase in Zn content from 0.5 to 1, the conversion of glycerol increased from 60.4% to 69.2 % and there is no appreciable change in selectivity towards glycerol carbonate. Further increase in Zn content to 1.5 conversion of glycerol decreased to 58.1%. Among the all, Zn_1TPA catalyst showed high activity compared to its counter parts. In order to know the efficiency of Zn_xTPA catalysts, turnover number (TON) were calculated and the corresponding values are presented in Table 2. The TON and selectivity towards glycerol carbonate depends upon the presence of Zn^{2+} ions in the secondary structure. The TON of pure TPA was low compared to Zn_xTPA catalysts. With the increase in Zn^{2+} content in TPA, the TON values increased and maximum value was obtained for Zn_1TPA catalyst.

The variation in the catalytic activity of Zn_xTPA catalysts can be explained based on the acidic properties of the catalysts. Activity of Zn_xTPA catalysts depended on the Zn^{2+}exchanged

with the protons of TPA. Partial exchange of TPA protons with Zn^{2+} results in generation of Lewis acidic sites along with Bronsted acidic sites. The high activity is mainly related to the presence of Lewis acidic sites originated from the presence of Zn in the secondary structure of TPA. The partial exchanged catalyst Zn_1TPA exhibited high activity as it contains more number of acidic sites.

Effect of catalyst calcination temperature on glycerol conversion

Zn_1TPA catalyst was calcined at different temperature in the range of 300–600 °C and studied for their activity for glycerol carbonate synthesis. The activity of catalysts are presented in Figure 6. From the figure it is noticed that with increase in calcination temperature from 300 to 600 °C, conversion of the glycerol decreased from 69.2 to 33.9%. Selectivity towards glycerol carbonate also followed the same trend. In order to know the variation in the catalytic activity and selectivity, these catalysts were further characterized by different spectroscopic techniques.

Characterization of Zn_1TPA catalyst calcined at different temperatures

XRD patterns of Zn_1TPA calcined at various temperatures are shown in Figure 7. Catalyst calcined at 300 °C, showed the characteristic peaks of Keggin ion as described earlier. Increase in calcination temperature to 400 °C, apart from the characteristic Keggin patterns additional peaks related to WO_3 were also observed.[40] This is due to partial decomposition of Zn_1TPA catalyst. In the case of catalyst calcined at 500 °C, no patterns related to Keggin ion was observed and patterns related to only WO_3 were observed. Further increase in calcination temperature to 600 °C, intense peaks related to crystalline WO_3 were noticed.[40] This indicates complete decomposition of Keggin ion at high calcination temperature. From the XRD results it can be concluded that Keggin structure of Zn_xTPA is thermally stable below 400 °C.

Stability of the Keggin ion of Zn_1TPA with increase in calcination temperature was further confirmed by Laser Raman spectroscopy. Figure 8 shows the Laser Raman spectra of Zn_1TPA catalyst calcined at various temperatures. Catalyst calcined at lower temperatures (300 and 400 °C) showed characteristic bands related to Keggin ion at 990 and 1011 cm^{-1} corresponding to asymmetric and symmetric vibration of $W=O_t$.[41] Whereas, catalyst calcined at higher temperatures (500 and 600 °C), bands related to Keggin ion were absent. New bands were observed at 824, 720, and 265 cm^{-1} which are characteristic bands of tungsten oxide.[40] These results suggest that Keggin ion of Zn_1TPA is decomposed to its constituent metal oxide at higher temperatures. These results are in agreement with the results obtained from XRD analysis.

TPD of ammonia patterns of Zn_1TPA catalyst calcined at various temperatures are shown in Figure 9. Catalyst calcined at 300 °C showed three unresolved peaks with high intensity. This indicates the presence of maximum acidity. Whereas, catalyst calcined at 400 °C showed two desorption peaks related to weak and strong acidic sites. The desorption peak related to moderate acidic sites was not observed for the catalyst calcined at 400 °C and exhibited low acidity compared to the catalyst calcined at 300 °C. This is due to partial degradation of Keggin units of Zn_1TPA at 400 °C. Further increase in catalyst calcination temperature up to 600 °C, there was no distinct ammonia desorption peak. This might be due to the complete decomposition of Zn_1TPA catalyst into its constituent metal oxide WO_3. From these studies it can be noted that catalyst with Keggin structure possess more number of acidic sites.

The high activity of the catalyst calcined at 300 °C is mainly due to presence of high acidity associated with the intact Keggin ion of Zn_1TPA. The catalyst calcined at high temperature showed low activity as their acidity decreased due to the decomposition of Keggin structure with temperature. The exchange of Zn^{2+} with the protons of TPA led to increased

acidity with the generation of Lewis acidic sites. Calcination of the catalysts at different temperatures results in variation of acidity with change in the structural characteristics.

Optimization of reaction parameters

Influence of the reaction time

Figure 10 shows the time on stream analysis of glycerol carbonate synthesis over Zn_1TPA catalyst at a reaction temperature of 140 °C. Conversion of glycerol carbonate increased continuously with time up to 6 h. Initially at 1 h of reaction time conversion of glycerol was only 38.7% and increased to 73.2% after 6 h of reaction time. However, glycerol carbonate selectivity was achieved maximum at 4 h of reaction time and decreased slightly at a longer reaction time.

Effect of reaction temperature

The effect of reaction temperature on conversion of glycerol and selectivity to glycerol carbonate are shown in Figure 11. Conversion of glycerol was very low (10%) when reaction was carried at below 120 °C. However, a drastic increase in the conversion of glycerol upto 69.2% was observed when reaction temperature increased to 140 °C. Selectivity towards glycerol carbonate also increased from 93.3 to 99.4% with increase in reaction temperature from 100 to 140 °C. Further increase in reaction temperature to 160 °C there is no appreciable increase in glycerol conversion, conversely selectivity towards glycerol carbonate was decreased.

Effect of glycerol to urea molar ratio

Glycerol to urea molar ratio is an important parameter to obtain high glycerol conversion and selectivity towards glycerol carbonate. Figure 12 shows the influence of glycerol to urea molar ratio. As shown in figure, the conversion of glycerol increased from 48.6 to 69.2% with decrease in glycerol to urea molar ratio from 2:1 to 1:1. The selectivity towards glycerol carbonate also increased upto 99.4%. Further decrease in glycerol to urea molar ratio there was

no marginal increase in the glycerol conversion and selectivity towards glycerol carbonate was decreased. The increase in selectivity towards by–product can be explained as follows: i) formation of glycedol due to decarbonylation of glycerol, ii) at higher concentration of urea, glycerol carbonate reacts with urea to give other by–product like (2–oxo–1,3–dioxolan–4–yl)methylcarbamate.[22] These results suggests that at moderate concentration of glycerol, the major product is glycerol carbonate.

Effect of catalyst weight

Figure 13 shows the effect of catalyst weight on the glycerol conversion and glycerol carbonate selectivity. Increase in catalyst loading from 3 to 5 % conversion of glycerol increased from 56.6 to 69.2 % and selectivity increased up to near 100 %. Further increase in catalyst loading from 5 to 10%, only a slight increase in glycerol conversion was observed and selectivity towards glycerol carbonate was decreased to 91.4% and formation of glycedol was observed. At high concentration of catalyst decarbonylation of glycerol carbonate favors to form glycedol. These results suggest that optimum loading of the catalyst is 5% to obtain high conversion of glycerol with high selectivity towards glycerol carbonate.

Reusability of catalyst

Recycling experiments were carried out to investigate the stability and reusability of the Zn_1TPA catalyst. In each cycle, the used catalyst was separated by filtration, washed with methanol to remove the products adhering to the surface of catalyst, dried in oven at 100 °C and reused for the next run. Figure 14 shows the reusability results of Zn_1TPA catalyst for the synthesis of glycerol carbonate. Fresh catalyst exhibited 69.2% of glycerol conversion and 99.4% selectivity for glycerol carbonate. The selectivity towards glycerol carbonate was almost constant in each recycle. However, a marginal decrease in glycerol conversion was observed

after third recycle of the catalyst. These results indicate the efficiency of the Zn_1TPA catalyst. Further studies are required to know the reasons for marginal decrease in activity.

Comparison of Zn_1TPA catalyst with reported solid acid catalysts

Table 3 shows the comparison of catalytic activity of Zn_1TPA catalyst with other reported solid acid catalysts. Gold supported on acidic supports such as Fe_2O_3 and Nb_2O_5 exhibited high conversion at high reaction temperature (150 °C).[42] However, the desired glycerol carbonate yield was very low. Sn-β zeolite exhibited 70% of glycerol conversion. The major drawback of this catalyst took long reaction time (5 h) for reasonable glycerol conversion. Among all the different solid acid catalysts zirconium phosphate exhibited 80% of glycerol conversion with 100% selectivity towards glycerol carbonate.[18] The high activity of this catalyst is due to presence of both acidic and basic sites. The present catalyst Zn_1TPA exhibited high glycerol conversion than previously reported catalysts such as tin-tungsten mixed oxide and Sm exchanged TPA catalysts.[14,24] Zn_1TPA catalyst exhibited about 69% glycerol conversion with near 100% selectivity towards glycerol carbonate. The present catalyst is reusable and exhibited high activity compared to other solid acid catalysts.

Conclusions

Zinc exchanged heteropoly tungstate catalysts prepared with retention of Keggin ion structure. Zn_xTPA catalysts are efficient catalysts for the synthesis of glycerol carbonate from glycerol and urea. The Zn_xTPA catalyst activity depends upon exchangeable Zn content which directs the overall acidity of the catalysts. Exchange of protons of TPA with Zn^{2+} resulted in generation of Lewis acidic sites along with Bronsted acidic sites. The acidity of the catalysts not only related to the amount of Zn in TPA but also its stability. High temperature calcination destabilized the Keggin ion of Zn_xTPA. Catalytic activity of Zn_1TPA also depends on reaction

temperature, catalyst loading and glycerol to urea molar ratio. The catalyst is reusable without any pre–treatment.

Acknowledgements

The authors thank to Council of Scientific Industrial Research (CSIR), India for the financial support in the form of Indus magic (CSC-0123) project under 12th Five Year Program.

References

1 M. Pagliaro, R. Ciriminna, H. Kimura, M. Rossi, C.D. Pina, *Angew. Chem. Int. Ed.* 2007, **46**, 4434–4440.

2 C.H. Zhou, J.N. Beltramini, Y.X. Fan, G.Q. Lu, *Chem. Soc. Rev.* 2008, **37**, 527–549.

3 A. Behr, J. Eilting, K. Irawadi, J. Leschinski, F. Lindner, *Green Chem.* 2008, **10**, 13–30.

4 D.T. Johnson, K.A. Taconi, *Environ. Prog.*, 2007, **26**, 338–348.

5 A.E.D. Alvarez, J. Francos, B.L. Barreira, P. Crochet, V. Cadierno, *Chem. Commun.,* 2011, **47**, 6208–6227.

6 Y. Gu, F. Jerome, *Green Chem.,* 2010, **12**, 1127–1138.

7 A. Tsuji, K.T.V. Rao, S. Nishimura, A. Takagaki, K. Ebitani, *ChemSusChem*, 2011, **4**, 542–548.

8 M. Balaraju, V. Rekha, B.L.A. Prabhavathi Devi, R.B.N. Prasad, P.S. Sai Prasad, N. Lingaiah, *Appl. Catal. A*, 2010, **384**, 107–114.

9 B. Katryniok, S. Paul, V.B. Baca, P. Reye, F. Dumeignil, *Green Chem.,* 2010, **12**, 2079–2098.

10 M.J. Climent, A. Corma, P.D. Frutos, S. Iborra, M. Noy, A. Velty, P. Concepcion, *J. Catal.,* 2010, **269**, 140–149.

11 J.R.O. Gomez, O.G.J. Aberasturi, B.M. Madurga, A.P. Rodriguez, C.R. Lopez, L.L. Ibarreta, J.T. Soria, M.C.V. Velasco, *Appl. Catal. A,* 2009, **366**, 315–324.

12 J. Hu, J. Li, Y. Gu, Z. Guan, W. Mo, Y. Ni, T. Li, G. Li, *Appl. Catal. A,* 2010, **386**, 188–193.

13 T. Mizuno, T. Nakai, M. Mihara, *Heteroatom Chem.*, 2010, **21**, 99–102.

14 K. Jagadeeswaraiah, Ch. Ramesh Kumar, P.S. Sai Prasad, S. Loridant, N. Lingaiah, *Appl. Catal. A,* 2014, **469**, 165–172.

15 C.G. Sancho, R.M. Tost, J.M.M. Robles, J.S. Gonzalez, A.J. Lopez, P.M. Torres, *Catal. Today,* 2011, **167**, 84–90.

16 M.O. Sonnati, S. Amigoni, E.P.T. de Givenchy, T. Darmanin, O. Choulet, F. Guittard, *Green Chem.,* 2013, **15**, 283–306.

17 J. Rousseau, C. Rousseau, B. Lynikaite, A. Sakcus, C. de Leon, P. Rollin, A. Tatibouet, *Tetrahedron,* 2009, **65**, 8571–8581.

18 M. Aresta, A. Dibenedetto, F. Nocito, C. Pastore, *J. Mol. Catal. A,* 2006, **257**, 149– 153.

19 T. Mizuno, T. Nakai, M. Mihara, *Heteroatom Chem.,* 2010, **21**, 541–545.

20 F.S.H. Simanjuntak, T.K. Kim, S.D. Lee, B.S. Ahn, H.S. Kim, H. Lee, *Appl. Catal. A,* 2011, **401**, 220–225.

21 J.B. Li, T. Wang, *J. Chem. Thermodyn.*, 2011, **43**, 731–736.

22 M. Okutsu, T. Kitsuki, WO Pat. 50415, 2000.

23 A.G. Shaikh, S. Sivaram, *Chem. Rev.*, 1996, **96**, 951–976.

24 Ch. Ramesh Kumar, K. Jagadeeswaraiah, P.S. Sai Prasad, N. Lingaiah, *ChemCatChem,* 2012, **4**, 1360–1367.

25 M. Aresta, A. Dibenedetto, F. Nocito, C. Ferragina, *J. Catal.*, 2009, **268**, 106–114.

26 C. Hammond, J.A.L. Sanchez, M.H.A. Rahim, N. Dimitratos, R.L. Jenkins, A.F. Carley, Q. He, C.J. Kiely, D.W. Knight, G.J. Hutchings, *Dalton Trans.,* 2011, **40**, 3927–3937.

27 C. Vieville, J. W. Yoo, S. Pelet, Z. Mouloungui, *Catal. Lett.,* 1998, **56**, 245–247.

28 G. Rokicki, P. Rakoczy, P. Parzuchowski, M. Sobiecki, *Green Chem.,* 2005, **7**, 529–539.

29 J.W. Yoo, Z. Mouloungui, *Stud. Surf. Sci. Catal.,* 2003, **146**, 757–760.

30 T. Okutsu, JP Pat. 039347, 2007.

31 J.H. Park, J.S. Choi, S.K. Woo, S.D. Lee, M. Cheong, H.S. Kim, H. Lee, *Appl. Catal. A,* 2012, **433–434**, 35–40.

32 F.R. Marcos, V.C. Casilda, M.A. Banares, J.F. Fernandez, *J. Catal.,* 2010, **275**, 288–293.

33 J. Li, X. Wang, W. Zhu, F. Cao, *ChemSusChem,* 2009, **2**, 177–183.

34 C.R. Kumar, N. Rambabu, N. Lingaiah, P.S.S. Prasad, A.K. Dalai, *Appl. Catal. A,* 2014, **471**, 1–11.

35 H. Yamamoto, *Proc. Jpn. Acad. Ser. B,* 2008, **84**, 134–146.

36 A. Corma, A. Martinez, C. Martinez, *J. Catal.,* 1996, **164**, 422–432.

37 D. Wang, S. Lu, P.J. Kulesza, C.M Li, R.D. Marco, S.P. Jiang, *Phys. Chem. Chem. Phys.,* 2011, **13**, 4400–4410.

38 G. Busca, J. Raman, *Spectroscopy,* 2002, **33**, 348–358.

39 Ch. Ramesh Kumar, P.S. Sai Prasad, N. Lingaiah, *J. Mol. Catal. A,* 2011, **350**, 83–90.

40 G. Liu, X. Wang, X. Wang, H. Han, C. Li, *J. Catal.,* 2012, **293**, 61–66.

41 T. Takashima, R. Nakamura, K. Hshimoto, *J. Phys. Chem. C,* 2009, **113**, 17247–17253.

42 Y. Ogasawara, S. Uchida, K. Yamaguchi, N. Mizuno, *Chem. Eur. J.,* 2009, **15**, 4343–4349.

Table 1 Acid strength distribution of Zn_xTPA catalysts.

Catalyst	Acidity (mmol/g)			
	Weak	Moderate	Strong	Total acidity
$Zn_{0.5}TPA$	0.513	0.032	1.866	2.411
Zn_1TPA	1.111	0.155	1.411	2.677
$Zn_{1.5}TPA$	0.071	0.927	0.563	1.561
Zn_1TPA–400	–	0.782	1.305	2.087
Zn_1TPA–500	–	0.184	0.005	0.189
Zn_1TPA–600	–	0.032	0.083	0.115

Table 2 Glycerol conversion and glycerol carbonate selectivity over Zn_xTPA catalysts.

Catalyst	Conversion of glycerol (%)	Selectivity (%)		TON
		Glycerol carbonate	others*	
TPA	40.4	75.7	24.3	126
$Zn_{0.5}TPA$	60.4	100	–	191
Zn_1TPA	69.2	99.4	0.6	221
$Zn_{1.5}TPA$	58.1	98.6	1.4	188
ZnO	34.0	91.2	8.8	31
Without catalyst	10.5	19.3	80.7	–

* 5–(hydroxymethyl)oxazolidin–2one, (2–oxo–1,3-dioxolan–4–yl)methylcarbamate, and glycedol.

Reaction conditions: Glycerol (2 g), Urea (1.306 g), Catalyst weight (0.2 g), Reaction temperature (140 ºC), Reaction time (4 h).

Table 3 Comparison of catalytic activity of the Zn_1TPA catalyst with other reported solid acid catalysts.

Catalyst	Reaction temperature (°C)	Reaction time (h)	Glycerol conversion (%)	Glycerol carbonate yield (%)	Ref.
Zn_1TPA	140	4	69.2	68.8	Present work
$Sm_{0.66}$TPA	140	4	49.5	42.3	[24]
SW21	140	4	52.1	49.7	[14]
Sn–β zeolite	145	5	70	26	[27]
Zr–P	140	3	80	76	[18]
Au/Fe_2O_3	150	4	80	39	[42]
2.5% Au/Nb_2O_5	150	4	66	21	[42]

Figure captions

Figure 1. XRD patterns of Zn_xTPA catalysts (a) TPA, (b) $Zn_{0.5}$TPA, (c) Zn_1TPA, and (d) $Zn_{1.5}$TPA.

(#) TPA, (*) ZnTPA.

Figure 2. FT–IR patterns of Zn_xTPA catalysts (a) TPA, (b) $Zn_{0.5}$TPA, (c) Zn_1TPA, and (d) $Zn_{1.5}$TPA.

Figure 3. Laser Raman spectra of spectra of Zn_xTPA catalysts (a) TPA, (b) $Zn_{0.5}$TPA, (c) Zn_1TPA, and (d) $Zn_{1.5}$TPA.

Figure 4. Temperature programmed desorption of ammonia profiles of Zn_xTPA catalysts (a) $Zn_{0.5}$TPA, (b) Zn_1TPA, and (c) $Zn_{1.5}$TPA.

Figure 5. Pyridine adsorbed FT–IR spectra of Zn_xTPA catalysts (a) TPA, (b) $Zn_{0.5}$TPA, (c) Zn_1TPA, and (d) $Zn_{1.5}$TPA.

Figure 6. Effect of Zn_1TPA catalyst calcination temperature on glycerol conversion.

Figure 7. XRD patterns of Zn_1TPA catalyst calcined at (a) 300 °C, (b) 400 °C, (c) 500 °C, and (d) 600 °C.

Figure 8. Laser Raman spectra of Zn_1TPA catalyst calcined at (a) 300 °C, (b) 400 °C, (c) 500 °C, and (d) 600 °C.

Figure 9. Temperature programmed desorption of ammonia patterns of Zn_1TPA catalyst calcined at (a) 300 °C, (b) 400 °C, (c) 500 °C, and (d) 600 °C.

Figure 10. Effect of reaction time on glycerol conversion and glycerol carbonate selectivity. **Reaction conditions:** Glycerol (2 g), Urea (1.306 g), Catalyst weight (0.2 g), Reaction temperature (140 ºC).

Figure 11. Effect of reaction temperature on glycerol conversion and glycerol carbonate

selectivity.

Reaction conditions: Glycerol (2 g), Urea (1.306 g), Catalyst weight (0.2 g), and Reaction time (4 h).

Figure 12. Influences of glycerol and urea molar ratio on glycerol conversion and glycerol carbonate selectivity.

Reaction conditions: Catalyst weight (0.2 g), Reaction temperature (140 ºC), and Reaction time (4 h).

Figure 13. Effect of catalyst weight on glycerol conversion and glycerol carbonate selectivity.

Reaction conditions: Glycerol (2 g), Urea (1.306 g), Reaction temperature (140 ºC), Reaction time (4 h).

Figure 14. Reusability of Zn_1TPA catalyst for carbonylation of glycerol.

Reaction conditions: Glycerol (2 g), Urea (1.306 g), Catalyst weight (0.2 g), Reaction temperature (140 ºC), Reaction time (4 h).

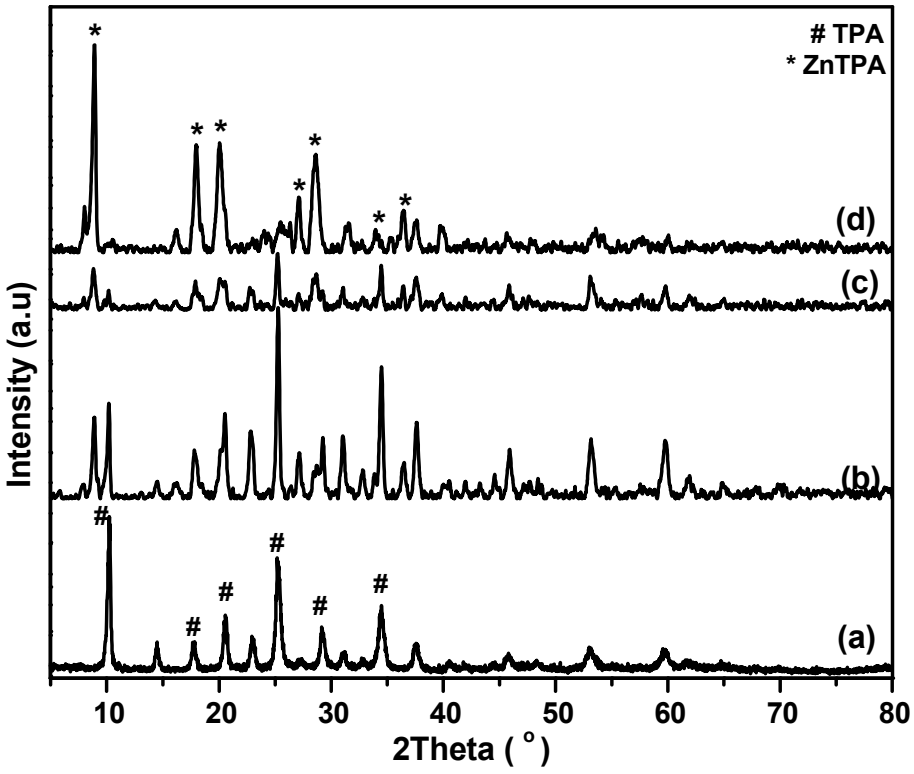

Figure 1

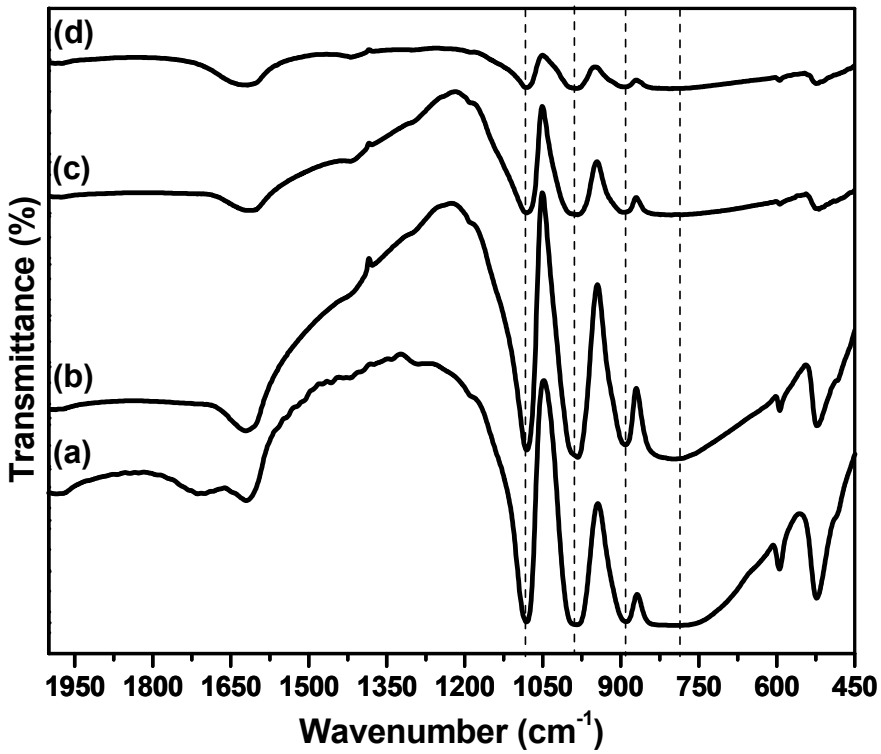

Figure 2

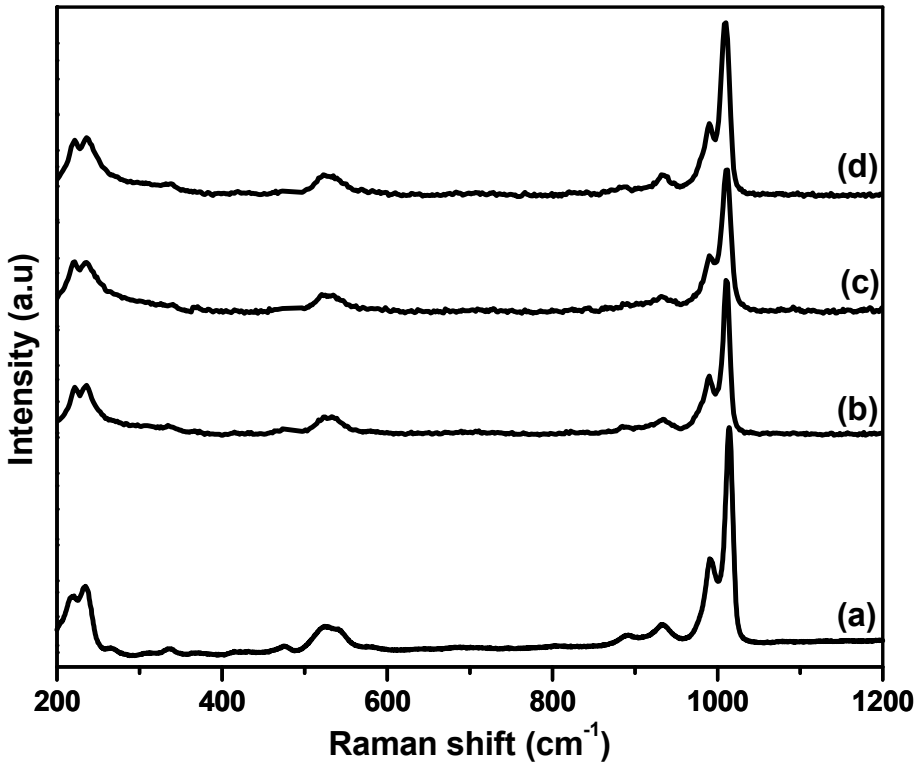

Figure 3

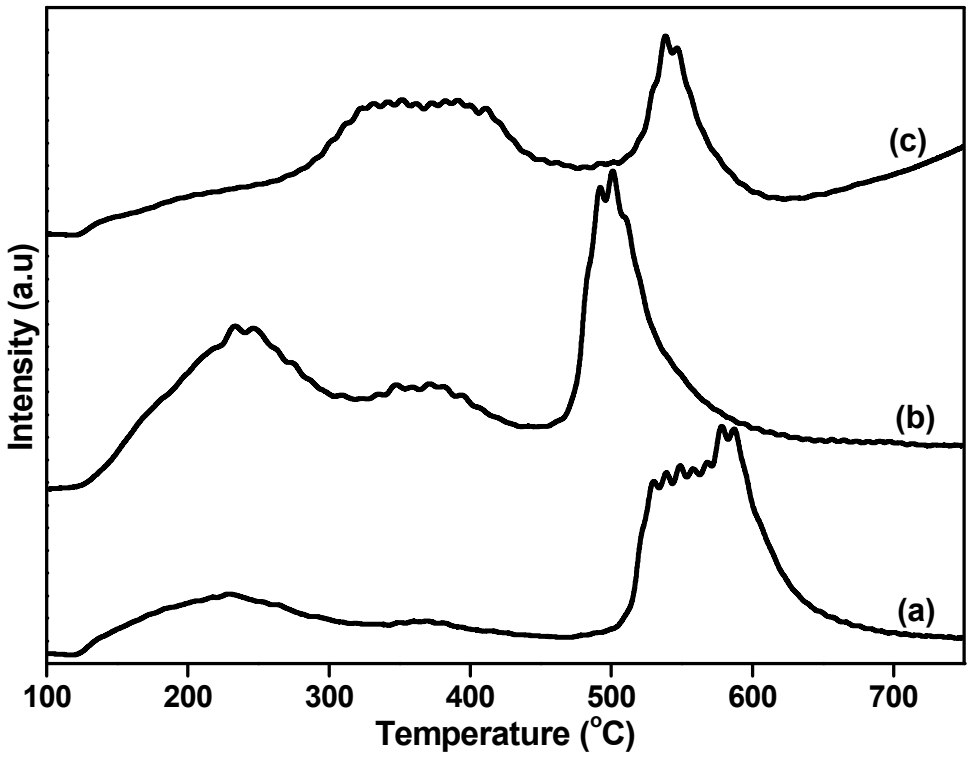

Figure 4

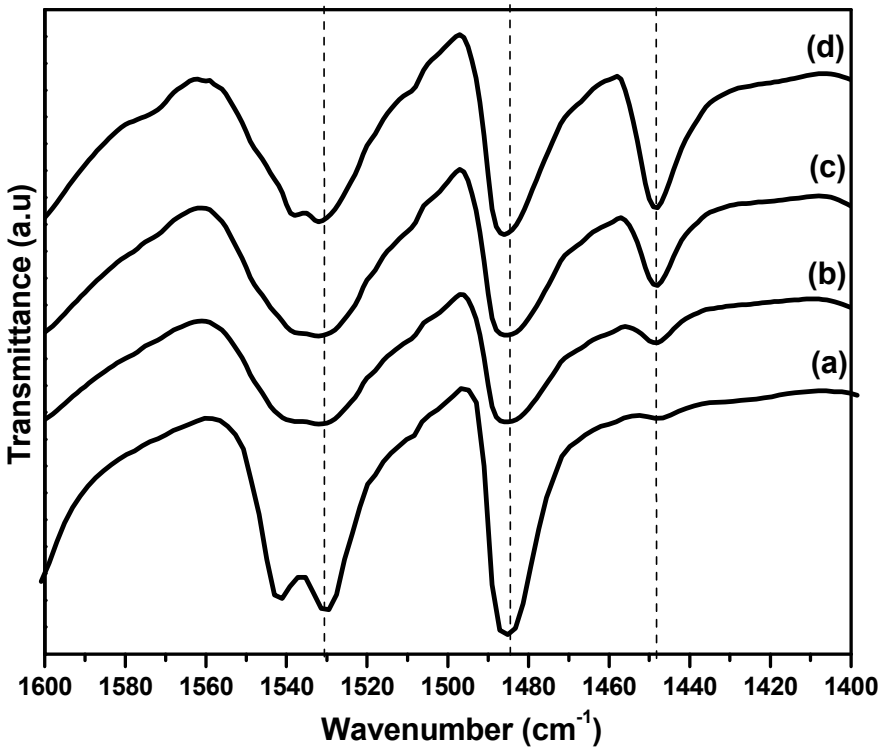

Figure 5

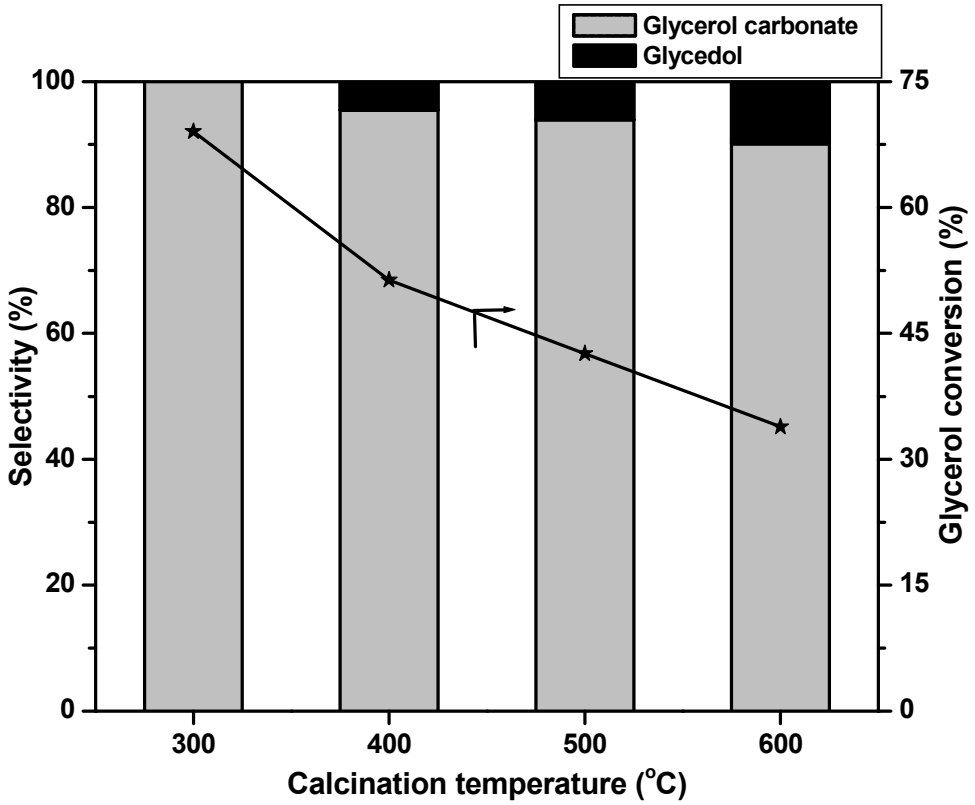

Figure 6

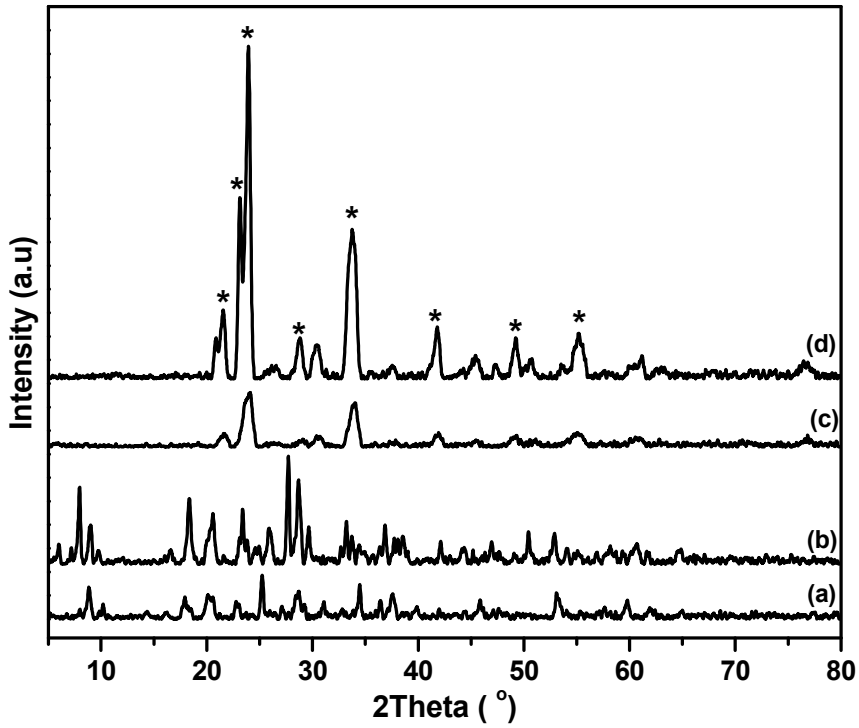

Figure 7

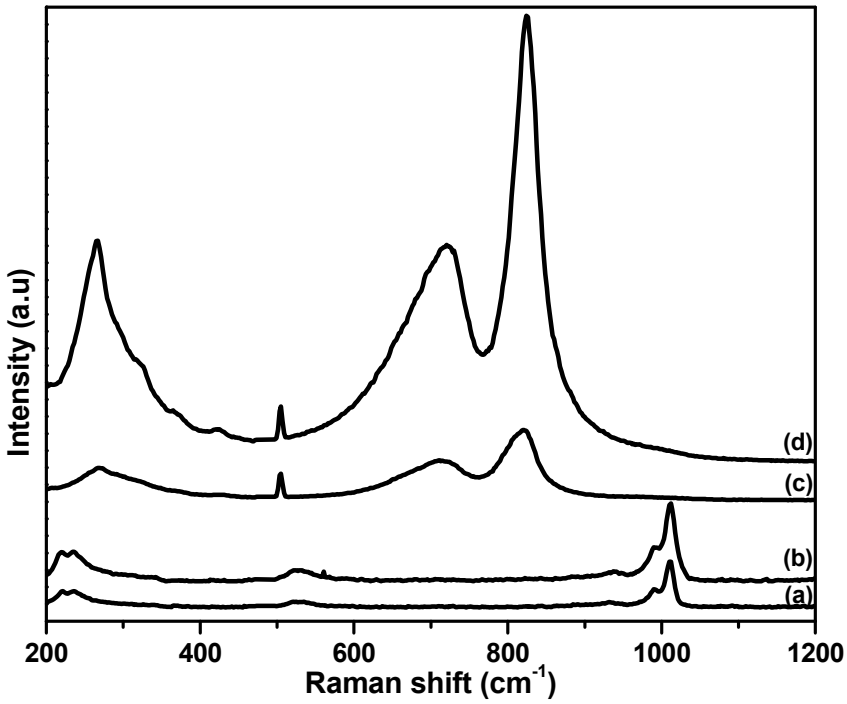

Figure 8

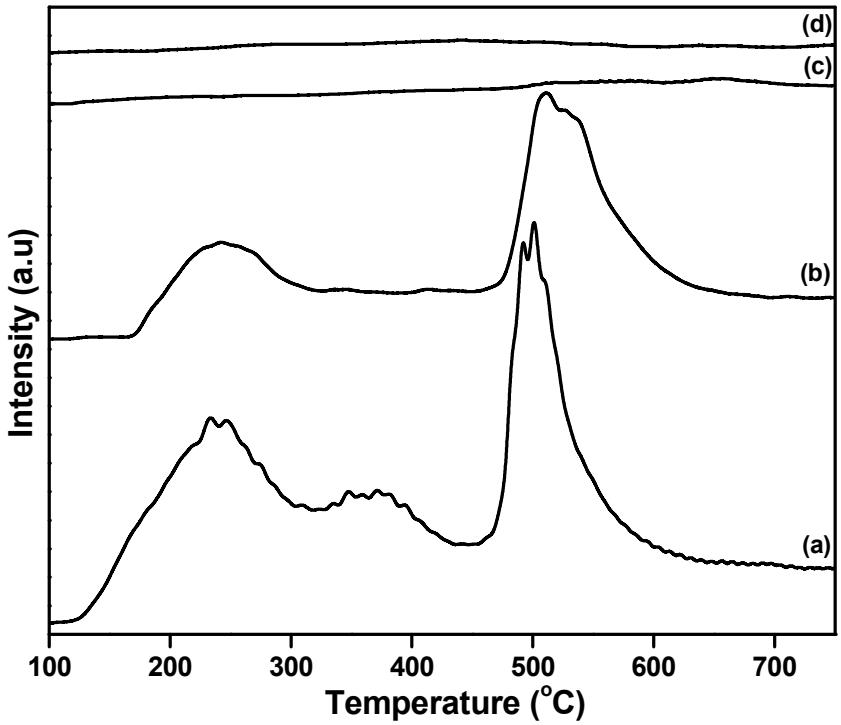

Figure 9

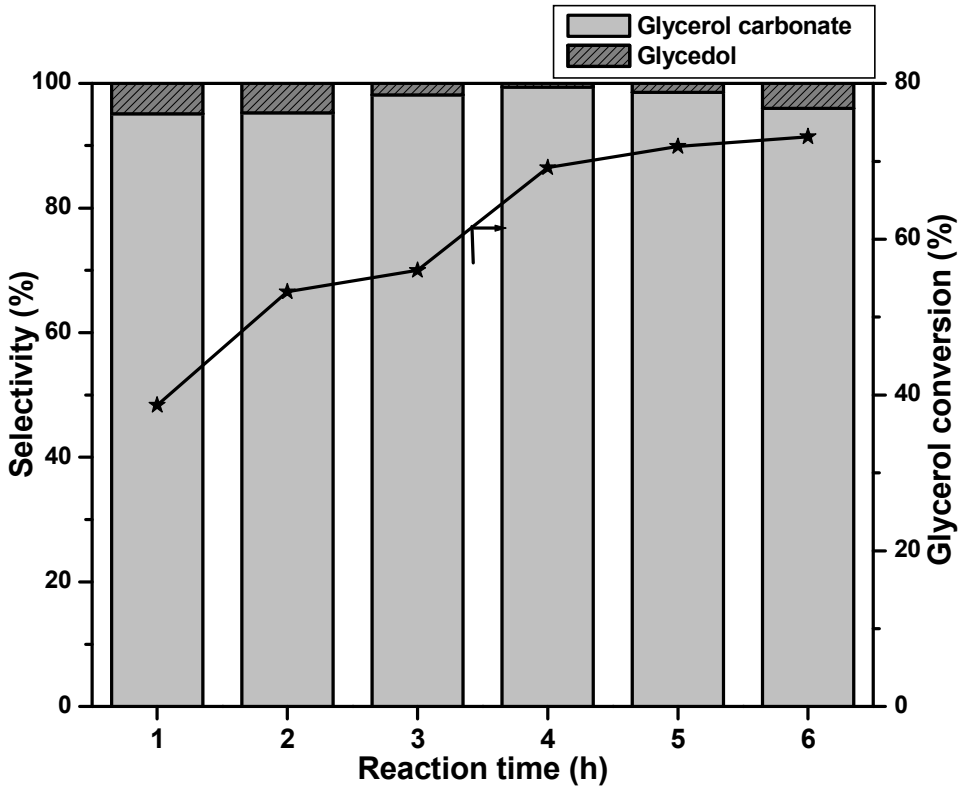

Figure 10

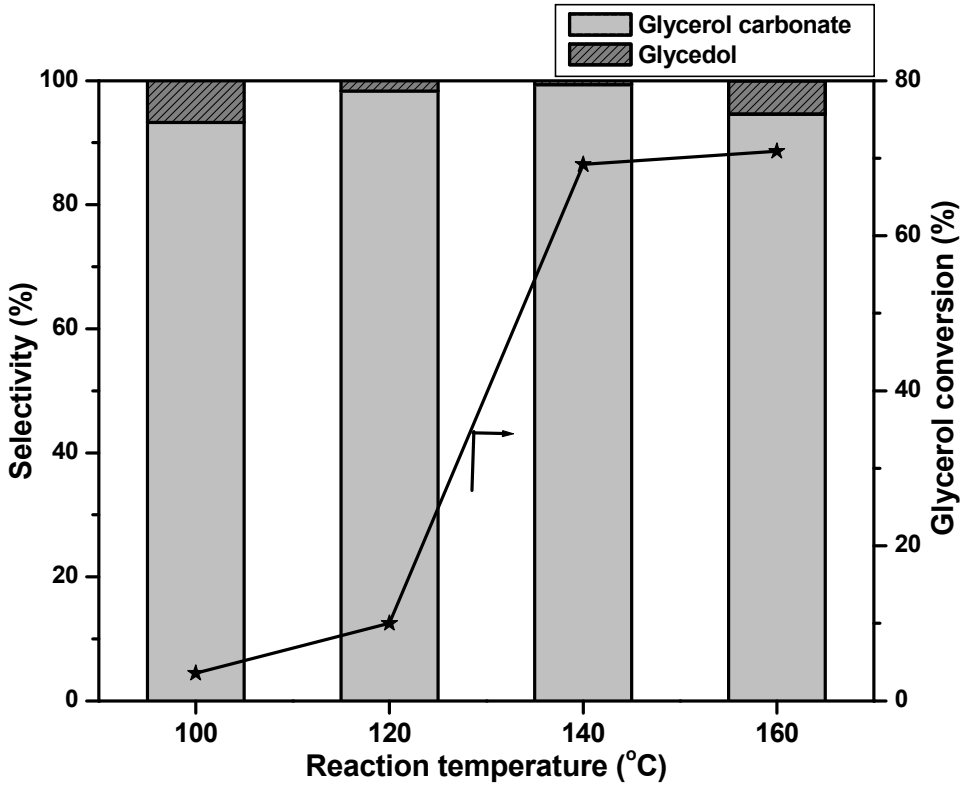

Figure 11

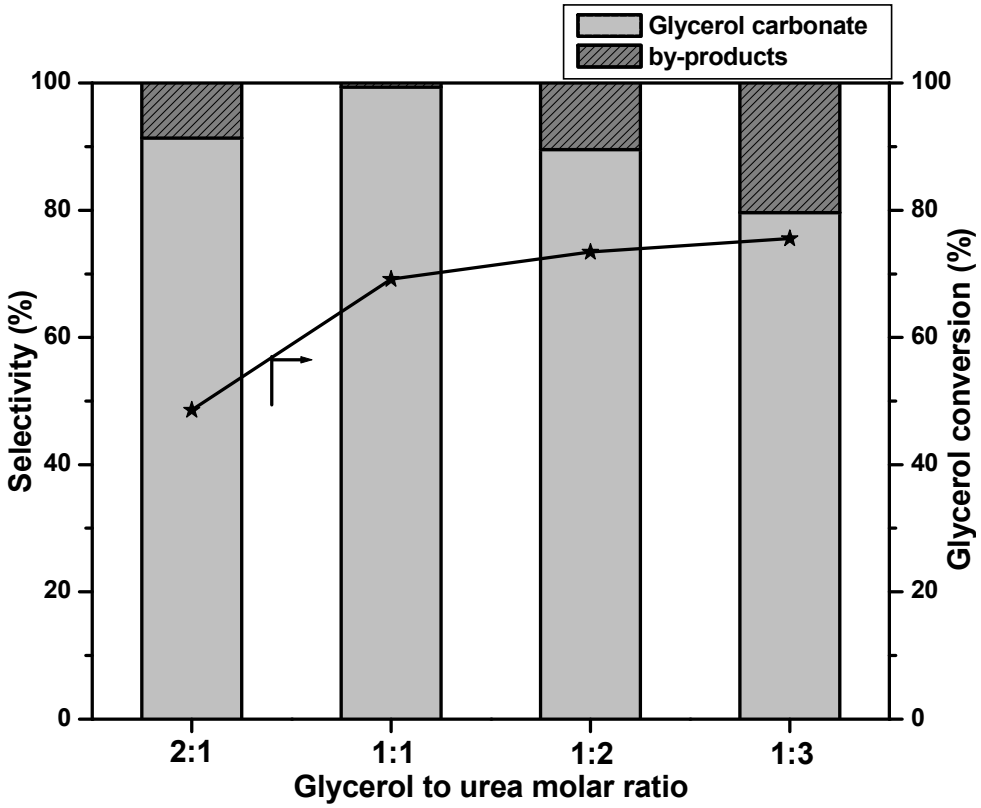

Figure 12

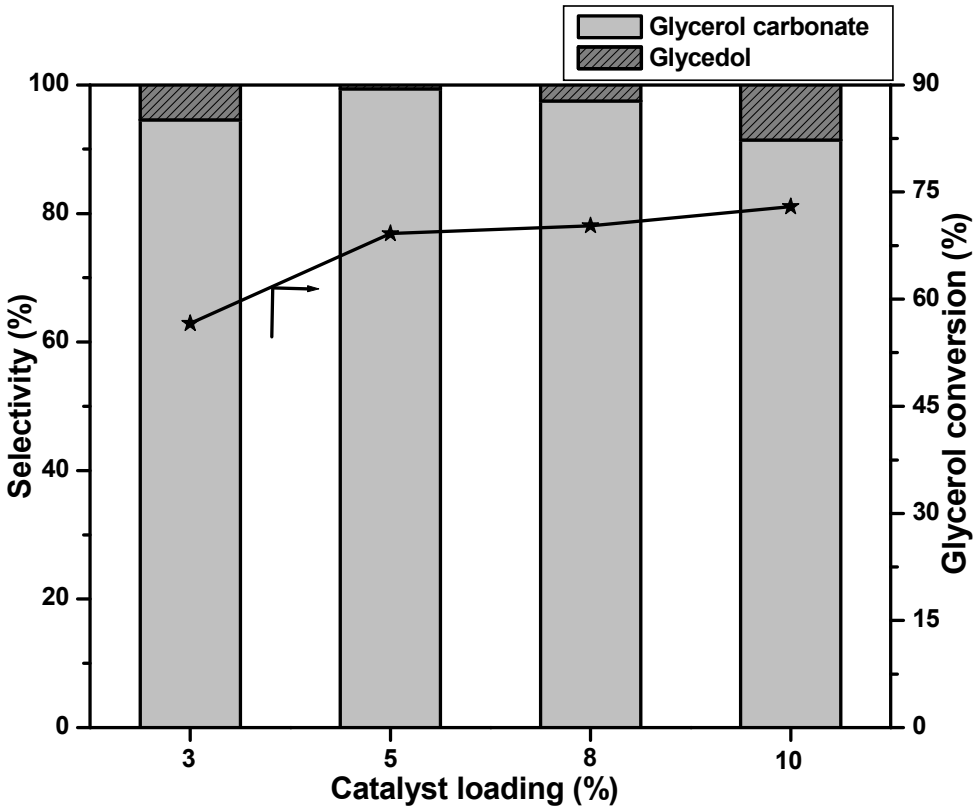

Figure 13

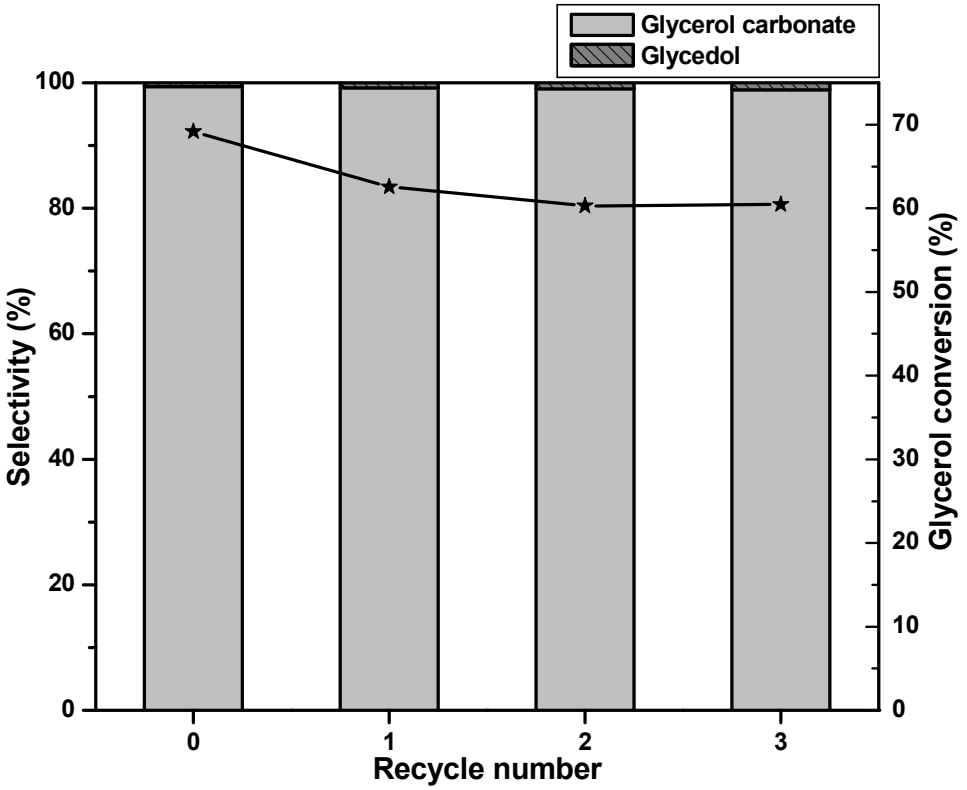

Figure 14